Factors Controlling Multiple Tropical Cyclone Events in the Western North Pacific*

JIANYUN GAO

Fujian Climate Center, CMA, Fuzhou, Fujian, China

TIM LI

IPRC and Department of Meteorology, University of Hawaii at Manoa, Honolulu, Hawaii

(Manuscript received 12 January 2010, in final form 26 July 2010)

ABSTRACT

The statistical feature of occurrence of multiple tropical cyclone (MTC) events in the western North Pacific (WNP) is examined during summer (June–September) for the period of 1979–2006. The number of MTC events ranged from one to eight per year, experiencing a marked interannual variation. The spatial distance between the TCs associated with MTC events is mostly less than 3000 km, which accounts for 73% of total samples. The longest active phase of an MTC event lasts for nine days, and about 80% of the MTC events last for five days or less. A composite analysis of active and inactive MTC phases reveals that positive low-level (negative upper-level) vorticity anomalies and enhanced convection and midtropospheric relative humidity are the favorable large-scale conditions for MTC genesis. About 77% of the MTC events occurred in the region where either the atmospheric intraseasonal (25–70 day) oscillation (ISO) or biweekly (10–20 day) oscillation (BWO) is in a wet phase. The overall occurrence of the MTC events is greatly regulated by the combined large-scale impact of BWO, ISO, and the lower-frequency (90 days or longer) oscillation. On the interannual time scale, the MTC frequency is closely related to the seasonal mean anomalies of 850-hPa vorticity, outgoing longwave radiation (OLR), and 500-hPa humidity fields. The combined ISO and BWO activity is greatly strengthened (weakened) in the WNP region during the MTC active (inactive) years.

1. Introduction

The western North Pacific (WNP) is the region of the most frequent tropical cyclone (TC) activity among eight TC genesis regions in the world (Gray 1968). Besides favorable summer mean conditions such as the monsoon trough and high sea surface temperature (SST), factors that affect TC genesis in WNP include precursor synoptic-scale disturbance signals (Fu et al. 2007) such as TC energy dispersion–induced Rossby wave trains (Li et al. 2003, 2006; Li and Fu 2006), easterly waves (Chang et al. 1970; Tam and Li 2006), and northwest–southeast-oriented synoptic wave trains unrelated to the energy dispersion of a preexisting TC (Lau and Lau 1990; Chang et al. 1996; Li 2006). Previous studies have reported a large-scale control of low-frequency systems on TC genesis (e.g., Nakazawa 1988; Liebmann et al. 1994; Harr and Elsberry 1995a,b; Chen et al. 2000; Maloney and Dickinson 2003; Camargo et al. 2007a,b; Ritchie and Holland 1999). For example, Liebmann et al. (1994) and Maloney and Hartmann (2000) found that the western and eastern Pacific TCs were modulated by the Madden–Julian oscillation (MJO). Lander (1994) and Wang and Chan (2002) showed that El Niño and La Niña may exert a great impact on the WNP TC activity. Yumoto and Matsuura (2001) found an interdecadal variation in the number of WNP TCs, which is somehow related to the Pacific decadal variability.

Observations show that TC formation is not a temporally evenly distributed event; rather, it has a tendency to cluster in some periods and be less frequent in other periods (Gray 1979). So far few studies have focused on TC clustering processes. In this paper we define a multiple tropical cyclone (MTC) event as an event in which two or more TCs form within a relatively short period. One example of such an MTC event in WNP is the successive cyclogenesis due to energy dispersion of a

* School of Ocean and Earth Science and Technology Contribution Number 8036 and International Pacific Research Center Contribution Number 729.

Corresponding author address: Dr. Jianyun Gao, Fujian Climate Center, CMA, Fuzhou, Fujian, China.
E-mail: brian.colle@stonybrook.edu

DOI: 10.1175/2010MWR3340.1

preexisting TC (Li and Fu 2006; Krouse and Sobel 2010). Another example is successive TC formation owing to energy accumulation of easterly waves at a critical longitude near the background confluence zone (e.g., Kuo et al. 2001). The objective of the present study is to document the statistical characteristics of MTC events in the WNP and examine the large-scale flow conditions under which an MTC event occurs. By analyzing the composite differences between the MTC active and inactive phases, we intend to understand the role of the atmospheric biweekly (10–20 day), intraseasonal (25–70 day), and lower-frequency (greater than 90 days) variabilities in regulating the MTC formation.

The rest of the paper is organized as follows. Section 2 describes the data and analysis methodology and the definition of multiple TC events. In section 3, we document the characteristics of the summer mean flow and biweekly (10–20 day) oscillation (BWO) and intraseasonal (25–70 day) oscillation (ISO) activity in association with MTC active and inactive phases. In section 4, we further investigate the interannual relationship between the MTC frequency and large-scale mean circulation including the seasonal mean fields and BWO and ISO intensity. A conclusion is given in section 5.

2. Data and methodology

a. Datasets

The primary datasets used in this study are the National Ocean and Atmospheric Administration (NOAA) outgoing longwave radiation (OLR; Liebmann and Smith 1996) and the National Centers for Environmental Prediction–Department of Energy (NCEP–DOE) Atmospheric Model Intercomparison Project (AMIP-II) Reanalysis (Kanamitsu et al. 2002). Both of the datasets are daily averaged products at a 2.5° × 2.5° grid, covered globally. The best-track TC data from the Joint Typhoon Warming Center (JTWC) are used to determine TC genesis time and location in the WNP. The typical warning of JTWC occurs when a TC just reaches the tropical depression intensity. The analysis period is confined in the summer months (June–September, when TCs are most active in WNP) from 1979 to 2006. Satellite products have been routinely incorporated into the NCEP assimilation system since 1979 (Kalnay et al. 1996).

A composite analysis method is utilized to reveal the difference of large-scale fields between MTC active and inactive phases. A Monte Carlo technique (Livezey and Chen 1983) is adopted to examine the statistical significance of the composite difference fields. A Lanczos filter (Duchon 1979) is applied to the daily OLR and reanalysis fields to extract the biweekly (10–20 day), intraseasonal (25–70 day), and lower-frequency (>90 days) components.

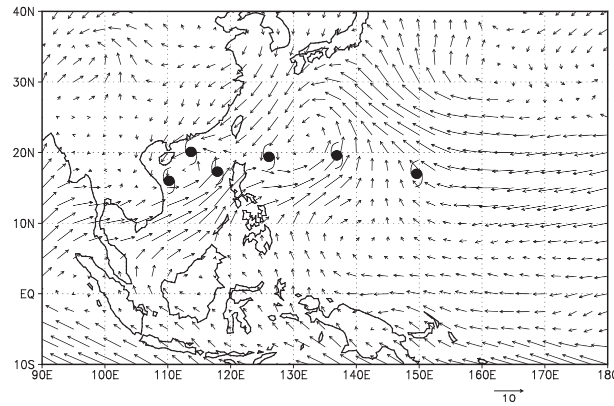

FIG. 1. TC genesis locations and averaged 850-mb wind patterns (vector) during an active MTC event on 10–18 Sep 1998.

b. Definition of multiple TC events

A variety of mechanisms may cause MTC (or TC clustering) events. From a synoptic self-triggering point of view, TC energy dispersion or wave energy accumulation in a confluence zone (e.g., Kuo et al. 2001; Li et al. 2003) may lead to the successive formation of TCs to the east of a preexisting TC. From a large-scale forcing point of view, the westward propagation of an active ISO or BWO event in WNP may cause the successive formation of TCs from east to west. Because of the complex forcing factors, the definition of an MTC event does not consider the relative location of TCs and is solely dependent on the genesis time. For a 28-yr period from 1979 to 2006, 483 TCs are identified in the peak summer season (June–September) over the WNP domain (2.5°–35°N, 100°E–180°).

A statistical calculation shows that an averaged interval of TC genesis in WNP during the summer (June–September) of 1979–2006 is 5.76 days. The TC genesis interval has a standard deviation of 5.13 days. A maximum interval of TC genesis in WNP is 37 days. A minimum interval is 0, which means that two or more TCs formed on the same day. In view of the statistical feature of the TC genesis dates, we stratify the MTC events into three categories: an MTC active phase (with a genesis interval being less than or equal to 3 days, that is, the mean interval minus half the standard deviation), an MTC inactive phase (with a genesis interval being greater than or equal to 9 days, that is, the mean plus half the standard deviation), and an MTC normal phase (with a genesis interval between 3 and 9 days). If two or more active (inactive) MTC phases occur successively, they are regarded as the same active (inactive) MTC event. Figure 1 shows an example of an active MTC event on 10–18 September 1998 during which six TCs formed in the WNP basin.

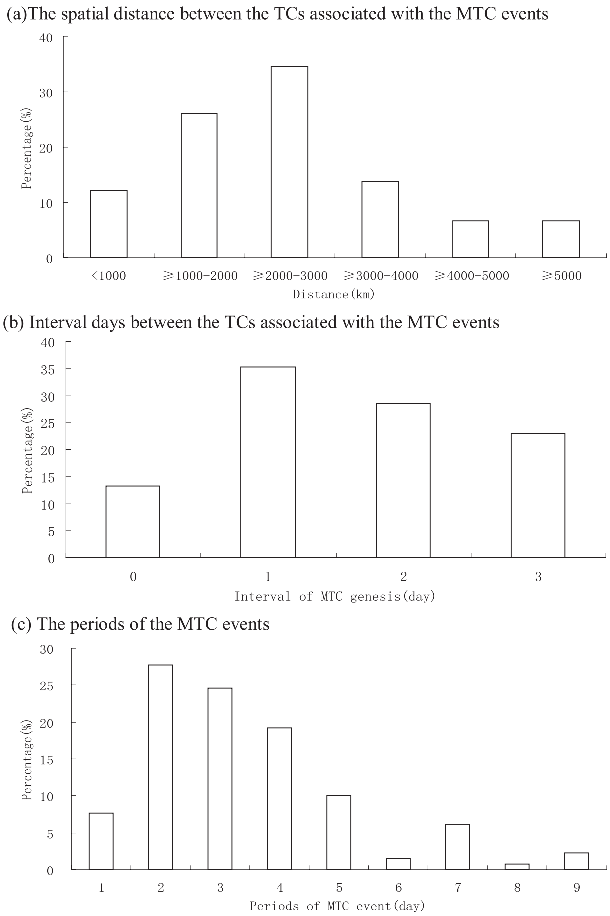

FIG. 2. The statistical characteristics of the MTC events in the WNP.

To examine the spatial and temporal distributions of MTC events in the WNP, we plotted the percentage occurrence of spatial distance between TCs that formed within the MTC events (Fig. 2a). It indicates that 73% of the MTC events have a distance less than 3000 km, while only 14% occur between 3000 and 4000 km and about 13% exceed a distance of 4000 km. About half of the TCs associated with the MTC events are only one day apart or less, and the other half have an interval of two and three days (Fig. 2b). Figure 2c shows that the longest active phase of an MTC event lasts for nine days, but about 80% of the MTC events last for five days or fewer.

Table 1 lists the criterion for the three MTC phases described above. It is seen from Table 1 that the numbers of the active, normal, and inactive MTC events for the 28-yr period are 130, 114, and 81, respectively. Thus the MTC active events occupied about 40% of the total samples. Although the MTC active phases covered only 446 days during the 28-yr period, 196 TCs formed in these active periods, which accounts for 41% of total TCs in the WNP.

TABLE 1. Stratification of three MTC phases based on the standard deviation σ of the TC genesis interval (TGI) in WNP (ATGI denotes the anomalous TC genesis interval).

Criterion		MTC phase	No. of events (%)
ATGI $\leq -0.5\sigma$	TGI $\leq$ 3 days	Active	130 (40%)
$-0.5\sigma <$ ATGI $< 0.5\sigma$	$3 <$ TGI < 9	Normal	114 (35%)
ATGI $\geq 0.5\sigma$	TGI $\geq$ 9 days	Inactive	81 (25%)

3. Composite analyses between the MTC active and inactive phases

Figure 3 illustrates individual active MTC events and associated TC genesis dates in the WNP during June–September for the period of 1979–2006. The gray bar in Fig. 3 represents the period of the active MTC event, while the black bar denotes each cyclogenesis date within the MTC event. No gap between the two black bars means that two TCs occur in successive dates. For each summer, the occurrence of the MTC events experiences a clear subseasonal variation. This suggests that the MTC events might be regulated by the atmospheric intraseasonal oscillation and biweekly oscillation.

In the following, a composite analysis is conducted to reveal the significant difference of dynamic and thermodynamic fields between the MTC active and inactive phases. The composite cases were selected based on the filtered daily data during the active and inactive MTC periods.

a. Difference of mean circulation patterns between MTC active and inactive phases

Figure 4 shows the differences of low-pass-filtered (90 days or longer) 850-hPa wind and vorticity, OLR, and 500-hPa relative humidity fields between the MTC active and inactive phases. The patterns of the composite wind and vorticity anomalies are approximately a mirror image between the active and inactive phases. A background low-level cyclonic (anticyclonic) circulation anomaly appears over the South China Sea (SCS) and WNP during the active (inactive) MTC periods. The anomalous circulation has a first baroclinic mode vertical structure, with an anticyclonic (cyclonic) circulation anomaly appearing in the upper troposphere (at 200 hPa) during the active (inactive) MTC phases (figure not shown). The WNP monsoon trough is strengthened and extends eastward during the active MTC periods, which favors MTC formation farther to the east.

The background dynamic fields are consistent with the OLR field (Fig. 4b). A significant difference in the tropical convection is found in WNP between the MTC

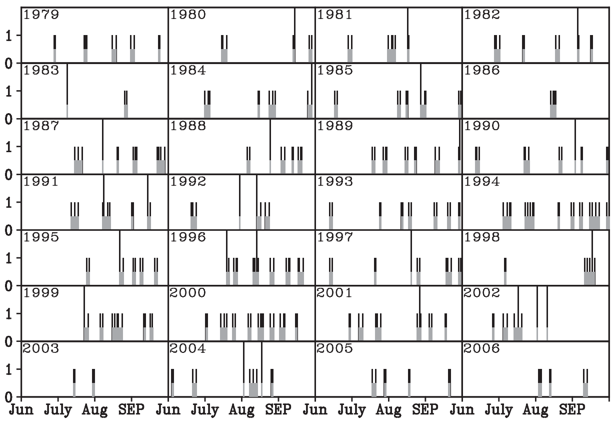

FIG. 3. Individual MTC active events (gray bar) and associated TC genesis dates and genesis number (black bar, with a short bar denoting one TC and a long bar denoting two TCs on the same date) during June–September 1979–2006.

active and inactive phases. Figure 4b illustrates that the convection is greatly strengthened south of 25°N along the WNP monsoon trough during the MTC active phase. In association with the enhanced monsoon convection, the relative humidity at 500 hPa increases significantly (Fig. 4c). The enhanced deep-layer moisture provides a favorable thermodynamic condition for the MTC genesis.

b. BWO and ISO activity associated with MTC active and inactive phases

How are the atmospheric BWO and ISO related to the occurrence of MTC events? Figure 5 shows the composites of 25–70-day bandpass-filtered OLR fields during the MTC inactive and active phase respectively. Note that during the MTC active phase negative OLR anomalies associated with ISO cover the entire SCS/WNP region from 110°E to east of 170°E and from 5° to 25°N. The condition is completely reverse in the MTC inactive phase, in which positive intraseasonal OLR anomalies occupy the region. The difference is statistically significant, exceeding the 95% confidence level. This indicates that ISO is in a wet (dry) phase with enhanced (suppressed) convective activity in WNP when an active (inactive) MTC phase occurs. This implies that the large-scale circulation anomaly associated with ISO favors the genesis of MTC events.

BWO, on the other hand, shows a different spatial pattern (Fig. 5). It is found that during the MTC active phase a negative OLR anomaly appears west of 140°E, while a positive OLR anomaly occurs to the east. The negative OLR anomaly to the west is stronger than the positive one to the east. Such a zonal dipole pattern is consistent with the fact that BWO has a relatively short zonal wavelength compared to that of ISO (Wen et al. 2010). An approximately opposite pattern of the OLR anomaly appears in the inactive MTC composite. The difference is most significant in a region from 125° to 140°E. The result suggests that the strengthened BWO activity in that region favors the MTC generation in WNP.

The possible effect of the large-scale control of ISO and BWO may be revealed by counting the percentage of individual MTC events that appear during the active phases of ISO and BWO respectively. Because of the spatial variability of cyclogenesis locations associated with the MTC events, the OLR values associated with ISO and BWO at individual genesis locations on the genesis dates were calculated. Prior to that, a Lanczos filter is applied to the daily OLR field to extract the biweekly (10–20 days), intraseasonal (25–70 days), and lower-frequency (>90 days) components. The number of positive and negative OLR values was then counted at each of the genesis location and date for each of the following scenarios: the ISO mode only, the BWO mode only, the sum of the ISO and BWO modes, and the sum of the ISO, BWO, and lower-frequency oscillation (LFO; >90 days) modes.

Table 2 shows the percentage of number of the negative OLR values during active MTC events for each of the scenarios above. It is found that about 77% of the TCs associated with the active MTC events occur when either BWO or ISO is in a wet phase. The combination of the BWO and ISO modes leads an increase of the occurrence percentage to 84%. This implies that the predictability of the MTC events might increase when one considers both the ISO and BWO impacts. The percentage of occurrence of the MTC events increases further to 98% when the combined BWO, ISO, and LFO forcing effects are included.

c. Synoptic-scale activity associated with MTC active and inactive phases

The composite analysis above reveals that positive low-level (negative upper level) vorticity anomalies and enhanced convection and midtropospheric relative humidity appear during the active MTC phase. The composite result may not indicate causal relationship. The large-scale condition in the MTC active composite may simply be reflecting the active presence of TCs in the period.

To address this issue, we conducted the following calculations. Assuming that TCs are a part of synoptic-scale (3–10 days) variability, if the accumulated synoptic effect significantly affects the mean flow, one would expect that the averaged synoptic-scale OLR value during

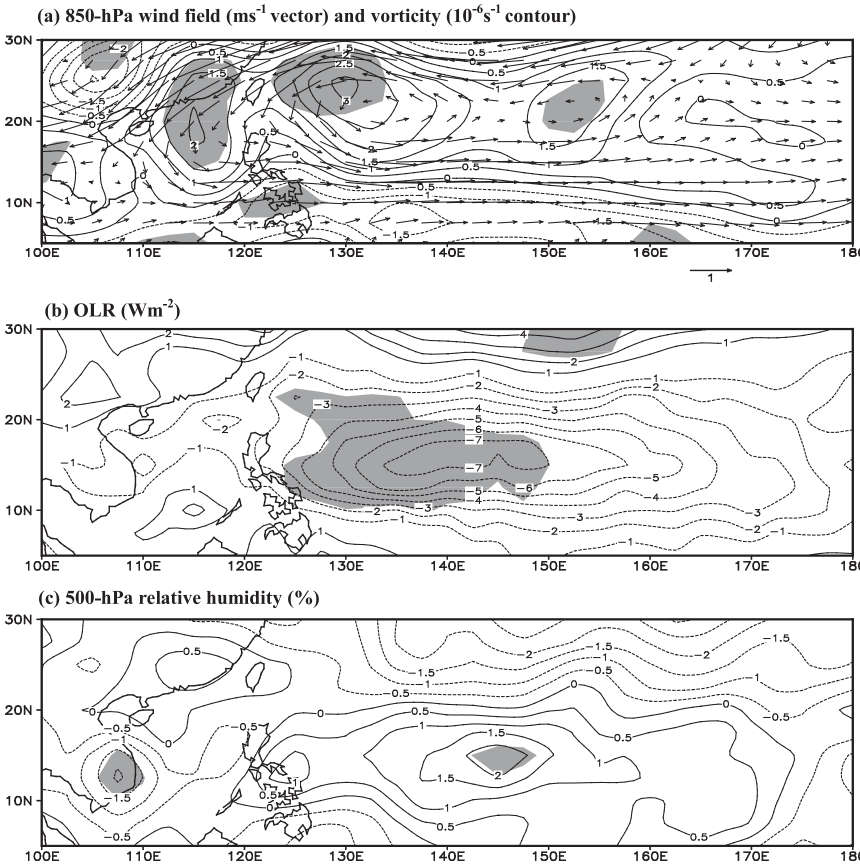

FIG. 4. Composite difference fields of (a) 850-hPa vorticity and wind, (b) OLR, and (c) 500-hPa relative humidity between MTC active and inactive phases. Shading indicates the area exceeding the 95% confidence level.

the active MTC phases should be much greater than the averaged value during the inactive MTC phases. Figure 6 shows that this is not the case. The averaged negative OLR value during the active MTC phase is not significantly larger than that during the inactive MTC phase. As a result, the averaged OLR values do not show a significant difference between the MTC active and inactive phases. The composite synoptic-scale OLR difference field is in a great contrast to the composite differences of the intraseasonal and lower-frequency OLR fields (Figs. 4 and 5). The result implies that the upscale feedback of the MTC events to the low-frequency oscillations is relatively weak. To the first order, it is the low-frequency motions that modulate the MTC formation.

4. Interannual variability of MTC frequency

The number of the MTC events each summer shows a notable interannual variation (Fig. 3). For example, the maximum MTC frequency is 8, which occurred in 2000. A minimum MTC frequency is 1, which happened in 1986. In the following we intend to identify significant large-scale fields associated with the interannual variability of the MTC frequency.

Figure 7 illustrates the correlations of the MTC frequency each summer with the 850-hPa vorticity, OLR, and 500-hPa humidity fields at various time scales. As one can see, the MTC frequency is significantly correlated with the seasonal mean vorticity and OLR fields in the large area of the WNP region. A high positive correlation coefficient with the vorticity and a high negative correlation coefficient with the OLR appear in the WNP monsoon trough region. For the ISO intensity, significant correlation appears in the region from 145° to 165°E and from 5° to 12°N in both the OLR and 500-hPa relative humidity fields. The correlation pattern appears different in the BWO intensity, with a positive correlation region extending from northwest (30°N, 120°E) to southeast (10°N, 160°E).

For the period of 1979–2006, the averaged number of the active MTC events per summer is 4.6, with a standard deviation of 1.7. Based on this statistical

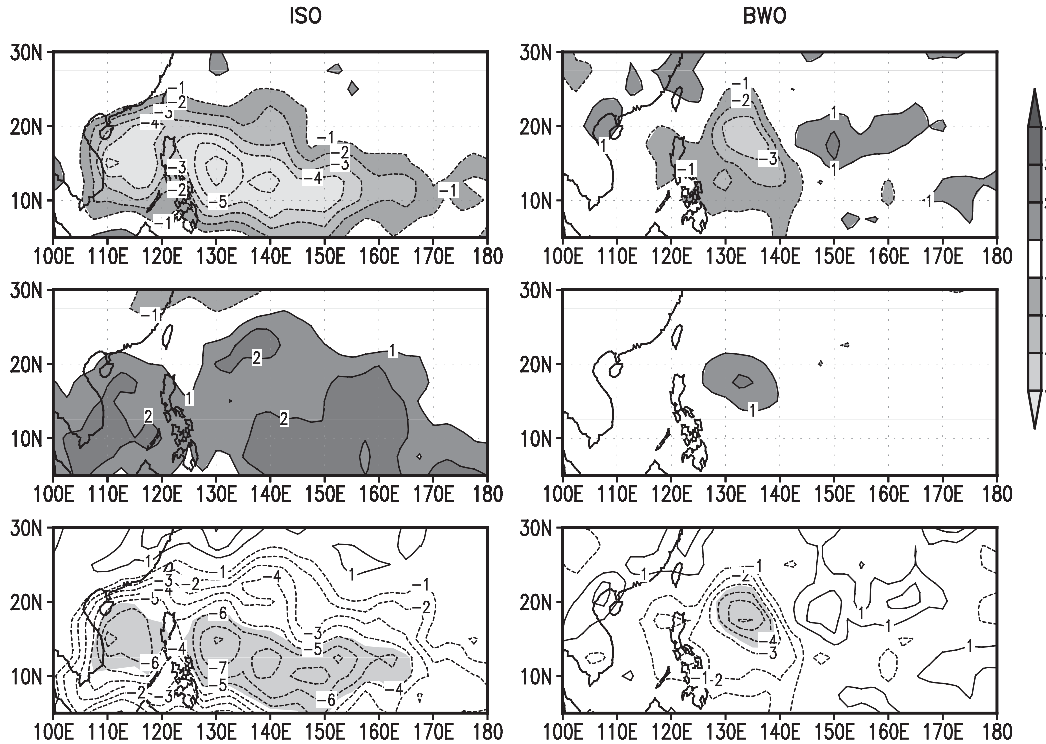

FIG. 5. The (left) 25–70-day and (right) 10–20-day bandpass-filtered OLR (unit: W m^{-2}) fields composed based on MTC (top) active and (middle) inactive phases and (bottom) their difference fields. The OLR anomalies with a value greater than (top) 1 W m^{-2} or less than (middle) −1 W m^{-2} are shaded. (bottom) Shading indicates the area exceeding the 95% confidence level.

feature, we define an MTC active year (when six or more MTC events occur), an MTC inactive year (when three or less MTC events occur), and an MTC normal year (when the number of the MTC events is between three and six). Based on this definition, nine active MTC years (2000, 1993, 1994, 1989, 1990, 1996, 1997, 2001, and 2004) and seven inactive MTC years (1980, 1981, 2006, 1983, 1998, 2003, and 1986) are selected for the subsequent composite analysis.

Figure 8 shows the composites difference of the ISO and BWO intensity between the MTC active and inactive years. Note that during the MTC active year, ISO is greatly enhanced over the equatorial region from 127° to 135°E and the off-equatorial WNP region from 130° to 165°E and from 5° to 20°N (Fig. 8a). The large-scale circulation pattern associated with the strengthened ISO convective activity may favor the genesis of the MTC events.

The BWO composite difference field, on the other hand, shows a different spatial pattern (Fig. 8b). In boreal summer, the BWO activity is primarily confined in the off-equatorial region, and is characterized by the northwestward propagation in the WNP (Li and Wang 2005). Figure 8b shows that the strengthened BWO activity extends from northwest (30°N, 120°E) to southeast (10°N, 160°E) during the MTC active years, compared to the MTC inactive years. The strengthened BWO activity may favor the MTC occurrence in the region.

The combined subseasonal large-scale forcing effect may be revealed by adding ISO and BWO intensity fields at each grid point. Figure 8c shows that the combined ISO and BWO intensity is greatly strengthened in the large area of the WNP region from 145° to 165°E and from 5° to 20°N during the MTC active years. This again implies that both the atmospheric ISO and BWO play an important role in regulating the MTC events.

TABLE 2. The percentage of occurrence of the MTC events in the genesis locations where BWO, ISO, and/or LFO are in a wet phase.

Mode	Percentage of occurrence of negative OLR values
BWO (10–20 days)	77.30
ISO (25–70 days)	76.69
BWO + ISO	84.05
BWO + ISO + LFO	97.85

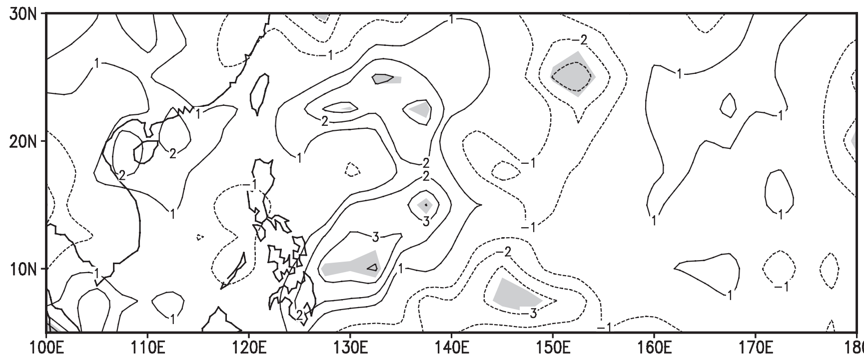

FIG. 6. Composite difference of the synoptic-scale (3–10 days) OLR field between the MTC active and inactive phases. Shading indicates the area exceeding the 95% confidence level.

5. Conclusions

In this study, we investigate the statistical feature of occurrence of observed multiple tropical cyclone (MTC) events in WNP. Using the JTWC best-track and the NCEP–DOE reanalysis data, we define the MTC active and inactive phases based on the statistics of TC genesis frequency in WNP. As an averaged TC genesis interval is 5.76 days in WNP, we stratify MTC events into three categories: an MTC active phase with a genesis interval being less than or equal to 3 days, an MTC inactive phase with a TC genesis interval being greater than or equal to 9 days, and an MTC normal phase with a genesis interval between 3 and 9 days. The number of

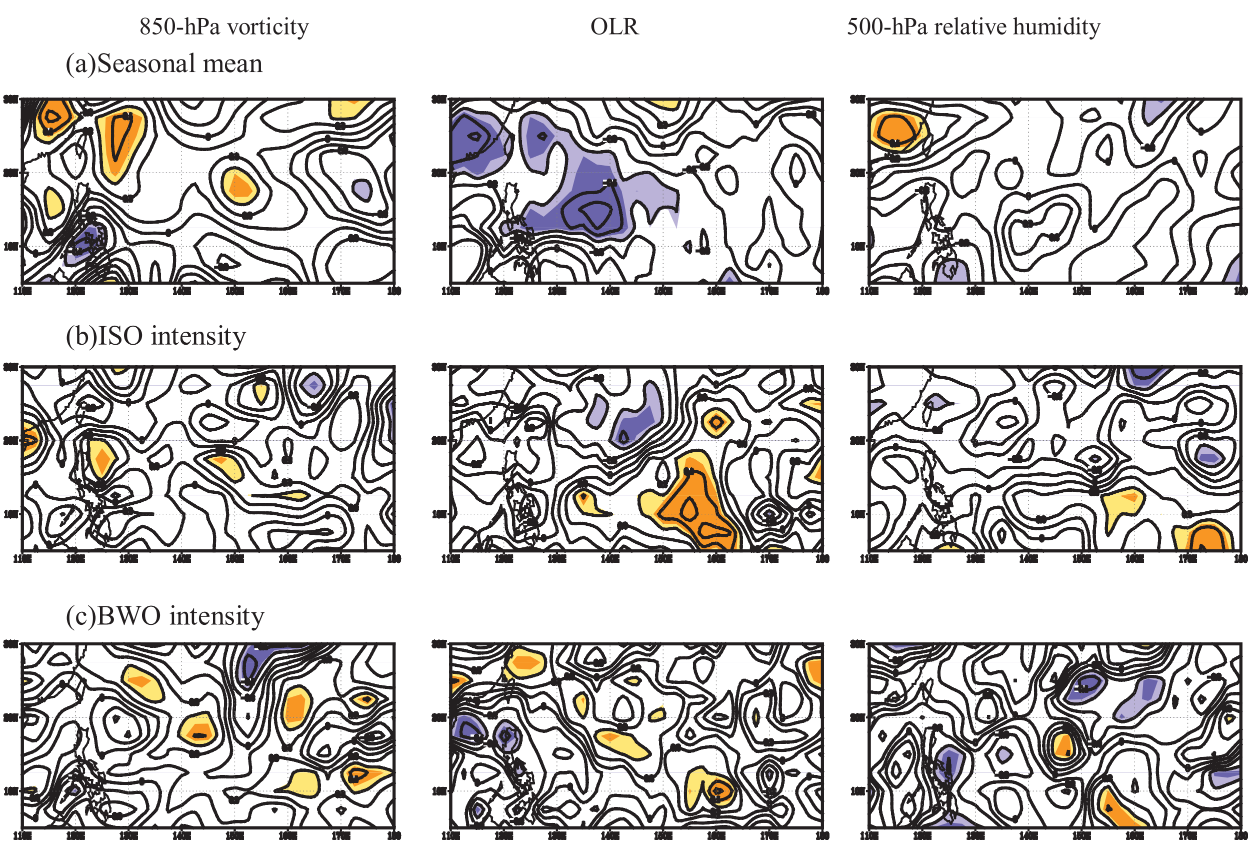

FIG. 7. Correlation coefficients of the summer MTC frequency with the seasonal mean (left) 850-hPa vorticity, (middle) OLR, and (right) 500-hPa relative humidity fields, and with the ISO and BWO intensity (represented by the standard deviation of 25–70-day and 10–20-day filtered fields, respectively). Shading indicates the area exceeding the 95% (darker color) and 90% (lighter color) confidence level.

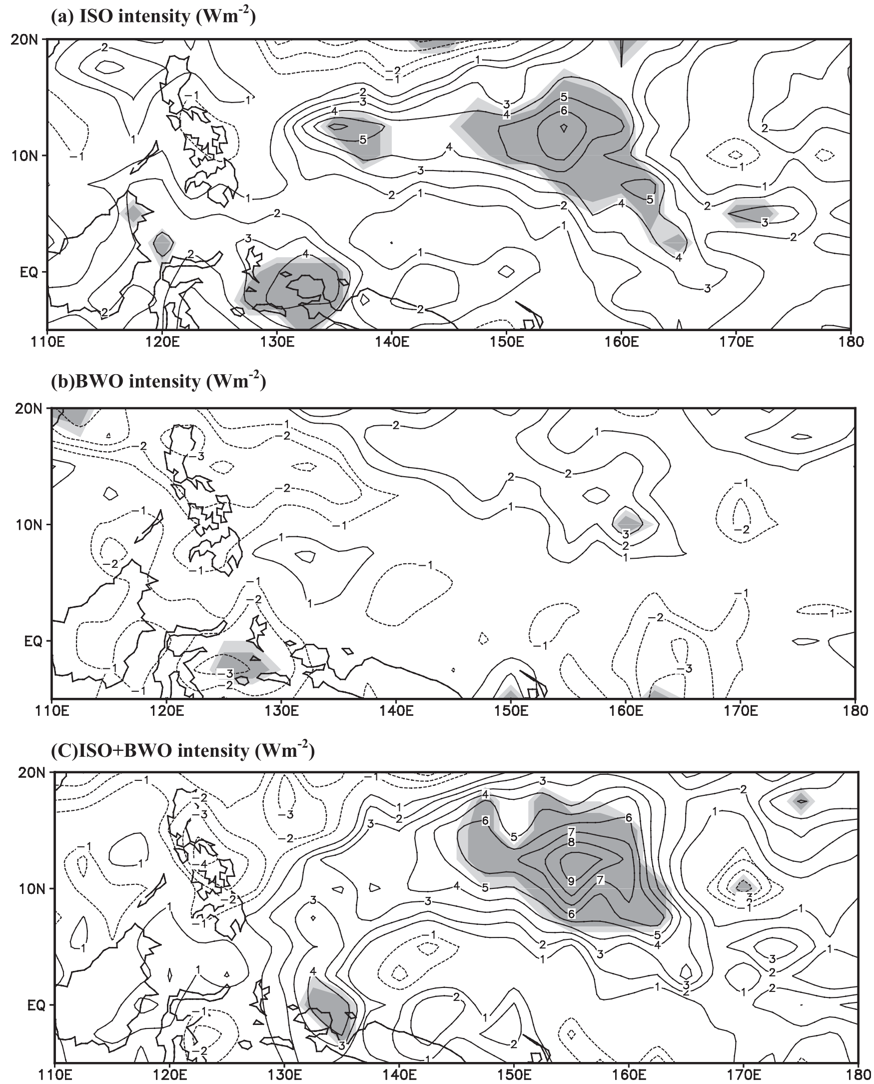

FIG. 8. Composite differences of (a) ISO intensity, (b) BWO intensity, and (c) the combined ISO and BWO intensity between the active and inactive MTC years. Shading indicates the area exceeding the 95% (darker color) and 90% (lighter color) confidence level.

so-defined active MTC events ranges from one to eight per year, experiencing a pronounced interannual variation. The overall numbers of the active, normal, and inactive MTC events for a 28-yr period (1979–2006) are 130, 114, and 81, respectively. The spatial distance between the TCs associated with MTC events is mostly less than 3000 km, which accounts for 73% of total samples. The longest active phase of an MTC event lasts for nine days. About 80% of the MTC events last for five days or fewer.

A composite analysis is further conducted to reveal the differences of the large-scale fields between the MTC active and inactive phases. The composite analysis reveals that the active MTC phase is associated with the enhanced low-level cyclonic and upper-level anticyclonic vorticity, enhanced monsoon convection, and the increase of midtropospheric relative humidity over SCS and WNP. An opposite pattern appears in the inactive MTC phase.

The occurrence of the summer MTC events is greatly regulated by the atmospheric biweekly and intraseasonal oscillations. It is found that about three quarters of individual MTC events occur in the region where either BWO or ISO is in a wet phase. On the other hand, the averaged synoptic-scale OLR value during the active MTC phase in the WNP is not significantly greater than that during the inactive MTC phase. The result implies that the upscale feedback of the MTC events to the low-frequency oscillations is relatively weak. To the first order, it is the low-frequency motions that modulate the MTC formation. The results suggest that the atmospheric low-frequency oscillations including BWO and ISO may modify the large-scale circulation in such a way that they create a favorable environmental condition for MTC genesis.

Our calculation shows that the combined large-scale impact of the ISO and BWO modes leads to an increase of the MTC occurrence percentage to 84%. The overall occurrence of the MTC events during the past 28 years is to a large extent determined by the combined effect of BWO, ISO, and the lower-frequency (90 days or longer) oscillation. Thus the current observational analysis sheds lights in the potential application of prediction of multiple tropical cyclone events in WNP.

On the interannual time scale, the MTC frequency shows a close relationship with the seasonal mean anomalies of 850-hPa vorticity, OLR, and 500-hPa humidity fields. A composite analysis shows a marked difference in the subseasonal variability between the MTC active and inactive years. The combined ISO and BWO activity is greatly strengthened (weakened) in the WNP region during the MTC active (inactive) years.

Acknowledgments. We thank anonymous reviewers for constructive comments that greatly improve the presentation of this paper. This work was done when JG visited IPRC. JG was supported by NSFC Grants 90915002 and 40775047 and by the youth project of Fujian Provincial Department of Science and Technology (2007F3019). TL was supported by ONR grants N000140810256 and N000141010774, NRL Grant N00173091G008 and the First Institute of Oceanography, and by the International Pacific Research Center, which is sponsored by the Japan Agency for Marine-Earth Science and Technology (JAMSTEC), NASA (NNX07AG53G), and NOAA (NA17RJ1230).

REFERENCES

Camargo, S. J., K. A. Emanuel, and A. H. Sobel, 2007a: Use of a genesis potential index to diagnose ENSO effects on tropical cyclone genesis. *J. Climate,* **20,** 4819–4834.

——, A. H. Sobel, A. G. Barnston, and K. A. Emanuel, 2007b: Tropical cyclone genesis potential index in climate models. *Tellus,* **59A,** 428–443.

Chang, C.-P., V. F. Morris, and J. M. Wallace, 1970: A statistical study of easterly waves in the western Pacific: July–December 1964. *J. Atmos. Sci.,* **27,** 195–201.

——, J. M. Chen, P. A. Harr, and L. E. Carr, 1996: Northwestward-propagating wave patterns over the tropical western North Pacific during summer. *Mon. Wea. Rev.,* **124,** 2245–2266.

Chen, T.-C., M.-C. Yen, and S.-P. Weng, 2000: Interaction between the summer monsoons in East Asia and the South China Sea: Intraseasonal monsoon modes. *J. Atmos. Sci.,* **57,** 1373–1392.

Duchon, C. E., 1979: Lanczos filter in one and two dimensions. *J. Appl. Meteor.,* **18,** 1016–1022.

Fu, B., T. Li, M. Peng, and F. Weng, 2007: Analysis of tropical cyclogenesis in the western North Pacific for 2000 and 2001. *Wea. Forecasting,* **22,** 763–780.

Gray, W. M., 1968: Global view of the origin of tropical disturbances and storms. *Mon. Wea. Rev.,* **96,** 669–700.

——, 1979: Hurricanes: Their formation structure, and likely role in the tropical circulation. *Meteorology over Tropical Oceans*, D. B. Shaw, Ed., Royal Meteorological Society, 155–218.

Harr, P. A., and R. L. Elsberry, 1995a: Large-scale circulation variability over the tropical western North Pacific. Part I: Spatial patterns and tropical cyclone characteristics. *Mon. Wea. Rev.,* **123,** 1225–1246.

——, and ——, 1995b: Large-scale circulation variability over the tropical western North Pacific. Part II: Persistence and transition characteristics. *Mon. Wea. Rev.,* **123,** 1247–1268.

Kalnay, E., and Coauthors, 1996: The NCEP/NCAR 40-Year Reanalysis Project. *Bull. Amer. Meteor. Soc.,* **77,** 437–441.

Kanamitsu, M., W. Ebisuzaki, J. Woolen, S.-K. Yang, J. J. Hnilo, M. Fiorino, and G. L. Potter, 2002: NCEP-DOE AMIP-II Reanalysis (R-2). *Bull. Amer. Meteor. Soc.,* **83,** 1631–1643.

Krouse, K., and A. Sobel, 2010: An observational study of multiple tropical cyclone events in the western North Pacific. *Tellus,* **62A,** 256–265.

Kuo, H.-C., J.-H. Chen, R. T. Williams, and C.-P. Chang, 2001: Rossby waves in zonally opposing mean flow: Behavior in the Northwest Pacific summer monsoon. *J. Atmos. Sci.,* **58,** 1035–1050.

Lander, M. A., 1994: An exploratory analysis of the relationship between tropical storm formation in the western North Pacific and ENSO. *Mon. Wea. Rev.,* **122,** 636–651.

Lau, K.-H., and N.-C. Lau, 1990: Observed structure and propagation characteristics of tropical summertime synoptic-scale disturbances. *Mon. Wea. Rev.,* **118,** 1888–1913.

Li, T., 2006: Origin of the summertime synoptic-scale wave train in the western North Pacific. *J. Atmos. Sci.,* **63,** 1093–1102.

——, and B. Wang, 2005: A review on the western North Pacific monsoon: Synoptic-to-interannual variabilities. *Terr. Atmos. Oceanic Sci.,* **16,** 285–314.

——, and B. Fu, 2006: Tropical cyclogenesis associated with Rossby wave energy dispersion of a preexisting typhoon. Part I: Satellite data analyses. *J. Atmos. Sci.,* **63,** 1377–1389.

——, ——, X. Ge, B. Wang, and M. Ping, 2003: Satellite data analysis and numerical simulation of tropical cyclone formation. *Geophys. Res. Lett.,* **30,** 2122–2126.

——, ——, ——, ——, and Y. Zhu, 2006: Tropical cyclogenesis associated with Rossby wave energy dispersion of a preexisting typhoon. Part II: Numerical simulations. *J. Atmos. Sci.,* **63,** 1390–1409.

Liebmann, B., and C. A. Smith, 1996: Description of a complete (interpolated) outgoing longwave radiation dataset. *Bull. Amer. Meteor. Soc.,* **77,** 1275–1277.

——, H. H. Hendon, and J. D. Glick, 1994: The relationship between tropical cyclones of the western Pacific and Indian Oceans and the Madden–Julian oscillation. *J. Meteor. Soc. Japan,* **72,** 401–412.

Livezey, R. E., and W. Y. Chen, 1983: Statistical field significance and its determination by Monte Carlo techniques. *Mon. Wea. Rev.,* **111,** 46–59.

Maloney, E. D., and D. L. Hartmann, 2000: Modulation of eastern North Pacific hurricane by the Madden–Julian oscillation. *J. Climate,* **13,** 1451–1460.

——, and M. J. Dickinson, 2003: The intraseasonal oscillation and the energetics of summertime tropical western North Pacific synoptic-scale disturbances. *J. Atmos. Sci.,* **60,** 2153–2168.

Nakazawa, T., 1988: Tropical super clusters within intraseasonal variations over the western Pacific. *J. Meteor. Soc. Japan,* **66,** 823–839.

Ritchie, E. A., and G. J. Holland, 1999: Large-scale patterns associated with tropical cyclogenesis in the western Pacific. *Mon. Wea. Rev.,* **127,** 2027–2043.

Tam, C., and T. Li, 2006: The origin and dispersion characteristics of the observed tropical summertime synoptic-scale waves over the western Pacific. *Mon. Wea. Rev.,* **134,** 1630–1646.

Wang, B., and J. C.-L. Chan, 2002: How strong ENSO events affect tropical storm activity over the western North Pacific. *J. Climate,* **15,** 1643–1658.

Wen, M., T. Li, R. Zhang, and Y. Qi, 2010: Structure and origin of the quasi-biweekly oscillation over the tropical Indian Ocean in boreal spring. *J. Atmos. Sci.,* **67,** 1965–1982.

Yumoto, M., and T. Matsuura, 2001: Interdecadal variability of tropical cyclone activity in the western North Pacific. *J. Meteor. Soc. Japan,* **79,** 23–35.